# A Computational Model of Ureteral Peristalsis and an Investigation into Ureteral Reflux

**G. Hosseini[1], C. Ji[2], D.Xu[2], M.A. Rezaienia[1],E.Avital[1], A. Munjiza[3], J.J.RWilliams[4],J.S.A Green[5,*]**

[1]School of Engineering and material sciences, Queen Mary University ofLondon, Mile End Road, London E1 4NS, UK; [2], Tianjin University, Tianjin, 200072, China.,[3]University of Split, 21000 ,Croatia[4] Sichuan University, Chengdu 610065, China,[5], Whipps Cross Hospital,London E11 1NR

## Abstract

The aim of this study is to create a computational model of the human ureteral system that accurately replicates the peristaltic movement of the ureter for a variety of physiological and pathological functions. The objectives of this research are met using our in-house fluid-structural dynamics code (CgLes-Ycode). A realistic peristaltic motion of the ureter is modelled using a novel piecewise linear force model. The urodynamic responses are investigated under two conditions of a healthy and a depressed contraction force. A ureteral pressure during the contraction shows a very good agreement with the corresponding clinical data. The results also show a dependency of the wall shear stresses on the contraction velocity. It confirms the presence of high shear stress at the proximal part of the ureter. Additionally, it is shown that an inefficient lumen contraction can increase the possibility of a continuous reflux during the propagation of peristalsis.

**Key words**: CFD, Ureter, Reflux, PUJ, VUJ, VUR

## 1 Introduction

The ureter is a muscular tube with non-linear mechanical properties, which conveys urine from the kidneys to the bladder [1]. In the urinary system, peristaltic motion is caused by a muscular contraction of the ureteral wall initiated by pacemakers. This drives urine from the kidney to the bladder through the ureter. Ureteral peristaltic motions are the result of a complicated movement of various differently aligned muscle fibres in the ureteral wall [2,3]. This is difficult to study experimentally since it is hard to analyse an individual muscle cell in isolation from its neighbours.

Mechanical properties of ureteral wall have been studied in many biomechanics research of soft biological tissues [1,4,5]. Yin et al [4] shows, ureteral wall has viscoelastic material properties and the stress strain relationship of the ureteral wall is nonlinear. Their result also shows that stress dose not only depended on the strain but also strain history. The history depended is related to hysteresis, stress relaxation and creep.

It is worthy of mention that the biomechanical properties and composition of the human ureter are affected by age and region-related [6]. According to the study by Sokolis et al [6], despite a non-significant difference between the left and right ureters, regional differences were established by the displacement of the stress –strain curves from the upper to lower ureter. The different distribution of the properties may be related to the difference in the functions. The stiffness, which increases distally, may constitute an adaptation of the ureter to its functional demands, namely storage of urine proximally where it is wider and distensible, and transfer of urine distally where the ureter is more resistant by being narrower and stiffer. Moreover, the collagen content of the upper ureter is increased by aging and it is distributed regional uniformly.

There is an increasing number of patients suffering from ureter diseases such as dysfunctional Pelvis Ureteric Junction (PUJ), Vesicoureteric reflux (VUR), and intrinsic and extrinsic obstruction the urinary tract infection. There is a wide range of clinical studies on the ureter, conducted in order to improve the understanding of urodynamic responses under different pathological conditions [7-11].

Several experimental techniques including x-ray screening, dynamic scintigraphy and Doppler ultrasonography have been used in previous studies to investigate urodynamic and ureteric peristalsis [12-20]. Kiil[20] used an invasive technique to measure the ureteral pressure using electronic strain-gauge pressure transducers attached to catheters inserted into the ureter.

Although the clinical data is more reliable, the non-controllable environment of an in vivo study as well as the invasive nature of the measurement procedure has encouraged many research groups to concentrate on numerical modelling of the ureter [21-27]. Recent advances in Computational Fluid Dynamic (CFD) and an increase in computing power make a realistic computational model of a ureter and peristaltic flow possible. Computational Fluid Dynamic (CFD) research also provides a tool for further develop and exploring this research problem. Kumar et al. [25] used the finite element method to investigate the influence of the magnitude of the Reynolds number, the wave amplitude and length on the urine flow. Their results indicated that progressive sinusoidal waves with high amplitude and low wave numbers caused peristaltic flows with high wall shear stress variations.

In a computational simulation of the ureteral system, when considering a series of basic assumptions , it may lead to less reliable results. The actual geometrical parameters, biomechanical properties, the origin of contractions and its multi-dimensional movements are important factors which were not considered in the majority of previous studies [21-26]. As a result, developing a computational platform which incorporates these factors will provide physicians with a better understanding of the exact mechanisms behind each disease, resulting in a better diagnosis and treatment.

One of the recent computational simulations of ureter was introduced by Vahidi et al. [27]. Cylindrical geometry with nonlinear material properties was simulated assuming a rigid contact surface in order to model the peristalsis. The result showed that recirculation regions formed against the jet flow, neighbouring the bolus peak. Through wave propagation, separation occurred behind the moving bolus on the wall and ureteropelvic reflux began from that location and extended upstream to the ureteral inlet. The maximum luminal pressure consistently occurred behind the urine bolus during the peristalsis. Their studies indicate that the function of ureteropelvic junction in prevention of reflux was significant.

Measuring the pressure pulses in the ureter is a key diagnostic tool to understand peristaltic activities. Intra-ureteral pressure has typically been studied using fluid filed catheters connected to a displacement type pressure transducer [10,19,20]. These pressure measurements rely on the movement of the urine in and out of a transducer chamber. However, in the absence of a catheter, the muscle contraction completely closes the cross-sectional area, so the pressure distribution over time is only a function of the muscle action and there will not be any fluid inside the closed lumen. Total contraction pressure is therefore solely a result of contact forces between the ureteral walls [28].

In our previous studies a simplistic cylindrical model of a ureter was simulated [29, 30]. The aim of this study is firstly to introduce a novel technique to simulate a realistic ureteral peristaltic contraction. For this study, the wall contact pressure in addition to the Intra-Abdominal Pressure (IAP) is used to investigate the pressure pulse. The pressure pulse was simulated by using the novel Piecewise Linear Force Model (PLFM) with the purpose of emulating the relaxation and contraction of individual muscles with fixed positions across time. To our knowledge, this technique has not been used in previous studies [20-27]. It is worth mentioning, this novel technique can be used in other simulations of other organs in cooperating a similar peristaltic movement such as human gastrointestinal tract.

Subsequently, a computational model of the ureteral system is accurately replicated and the peristaltic movement in two conditions of a healthy and a depressed contraction force is investigated. The simulations are carried out using our in-house CFD platform, known as CgLes [31,32] to model the urine flow, coupled with our in-house structural code, known as Y code [33] to model viscoelastic ureteral wall. CgLes is a three-dimensional fluid solver with a second order accuracy in both time and space and is based on a finite volume formulation. The capability of CgLes to simulate both laminar and turbulent flows has been extensively verified [32]. Y code uses the combined finite discrete element method to simulate the deformation of solid structure [33].

# 2 Methodology

## 2.1 A Solver for Incompressible Viscous Flow (urine):

For the fluid phase, urine is modelled as an incompressible viscous flow which can be described by the Navier-Stokes equations. The Navier–Stokes equations for incompressible viscous flows are described in equation 1.

$$\rho\left[\frac{\partial u_i}{\partial t}+\frac{u_i u_j}{\partial x_j}\right]=-\frac{\partial p}{\partial x_i}+\mu.\frac{\partial^2 u_j^2}{\partial x_j \partial x_j}+f \qquad (1)$$

Where u is the vector of fluid velocities, *p* is the pressure, $\mu$ is dynamic viscosity and *f* is a body force term. For time-stepping, the 2nd order Adams-Bash method used. The Navier-Stokes equations are discretised on a fixed staggered Cartesian grid by the finite volume approach. The spatial derivatives in the diffusion and convection terms are approximated using the second order finite volume method. A conjugate gradient method is used to solve the pressure Poisson equation which is resulted from the time-fractional method used to ensure continuity [32,34].The fluid domain is created by 213 blocks with the grid resolution of 64 × 448 × 960 points. The grid cell length in the x, y and z directions is 0.0078 ×0.0089 ×0.02 cm, respectively.

## 2.2 A Solver for the Deformation of the Solid (ureter):

For the solid phase, the combined finite-discrete element method is used to simulate the movement and deformation of the ureter under external forces [33]. The equation of motion is solved by an explicit time integration scheme based on a central difference method of second order.

The static shape of a healthy human ureter was obtained by using CT scans of the urinary system of a female human. The CT scans were imported into the image-processing package Mimics (14.01) to convert them into a 3D model as shown in Figure 1(a). The centre line of the 3D geometry was obtained using Mimic software and the resulting 3D model gave a fair approximation of the ureter's geometry. The length and the average diameter of the ureter are 22 cm and 0.5 cm respectively.

For this study, Ansys ICEM 15.0 was used to create the tetrahedral mesh for the structural model. There are 6700 elements, 1891 nodes in the structural model. The minimum and maximum element sizes are 0.005 cm and 0.7 cm respectively. Figure 1(b) shows the combined fluid and solid domains.

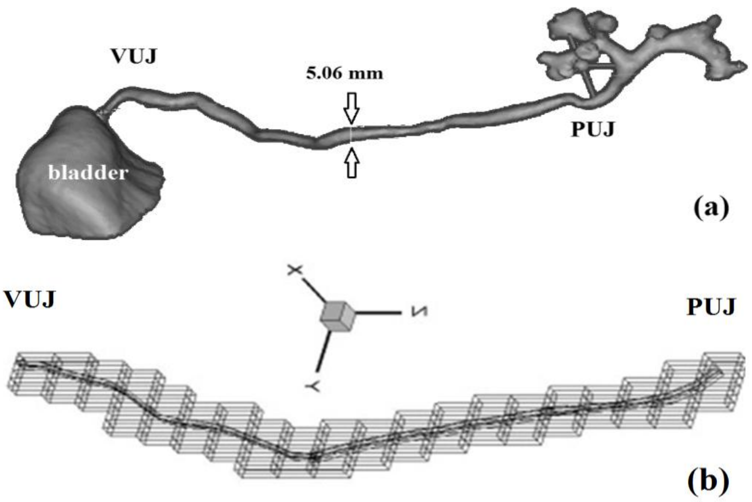


Figure 1(a): Cropped 3D model of the right ureter and bladder, (b):The combined fluid and solid domains of the ureter.

## 2.3 Ureteral Wall Properties:

To mimic a realistic computational model of ureteral wall, the non linear tensile properties of the ureter have to be considered. To adapt the nonlinear tensile properties of the ureter, a scalar quantity called "Equivalent strain (EQ''is introduced into the structural code. This is described in Eq (2) where $\boldsymbol{v = 0.35}$ is Poisson ratio, $\varepsilon_{11}$, $\varepsilon_{22,}$ $\varepsilon_{33}$ are principal strains and $\varepsilon_{12}$, $\varepsilon_{23,}$ $\varepsilon_{31}$ are shear strains from the strain tensor E. By implementing the equivalent strain into the structural code, multiple strains in the computational model become equivalent to the uniaxial strain reported in the experimental study [2].

$$\varepsilon_v = \frac{1}{1+v} \sqrt{\frac{\left(\varepsilon_{11} - \varepsilon_{22}\right)^2 + \left(\varepsilon_{22} - \varepsilon_{33}\right)^2 + \left(\varepsilon_{11} - \varepsilon_{33}\right)^2 + 6\left(\varepsilon_{12}^2 + \varepsilon_{23}^2 + \varepsilon_{31}^2\right)^2}{2}} \quad (2)$$

As shown in Figure 2, an exponential function was obtained where the best fitted function from the stress-strain curve by Yin & Fung [2] was used, and implemented in the structural code.

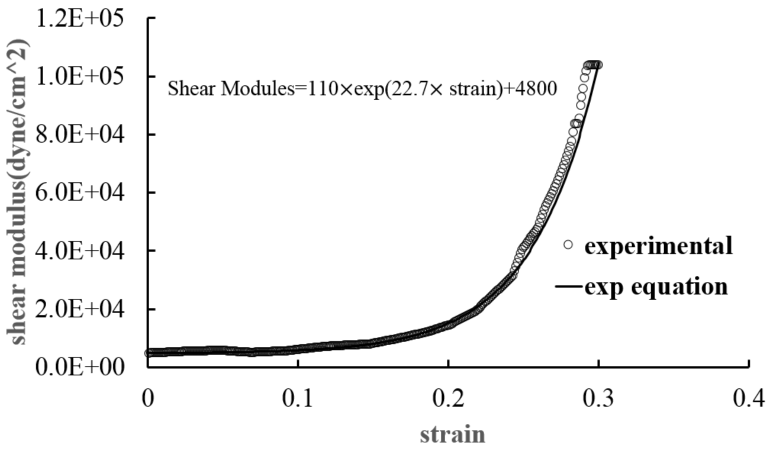


Figure 2: The non-linear stress-strain relationship of the ureteral wall data, extracted from Yin and Fung [2] and an exponential function matched to this data and implemented in the structural code.

## 2.4 Immerse Boundary:

To couple the fluid motion and solid deformation, an Immerse Boundary (IB) method was used to link the interface between the fluid and the solid, both of which have independent meshes. By introducing a force term into the fluid's momentum equations, the IB points become non-slip boundary points. A spatially second order direct-forcing scheme was used for the implementation of the IB method. The combined code has been verified in previous studies [29,30,32,34] for a range of engineering problems from sediment flow to fluid-structure interaction in a pipe.

## 2.5 Piecewise Linear Force Model:

The ureteral peristaltic contraction was simulated using the novel Piecewise Linear Force Model (PLFM) with the purpose of emulating the relaxation and contraction of individual muscles with fixed positions across time.

ThePLFM is shown in Eq (3) *m* is the total number of sections of the contraction. The two other variables are *s* and *t* where *s* is defined as the point in time at which a contraction is transferred from one cross-section to another cross-section of the ureter. *t* is the time at the beginning of the window for each cross-section. The force function, which acts on each cross-section in this contraction model, is given in Eq (3).

$$F(t) = \begin{cases} \frac{F_{max}}{s} t, & 0 < t < s \\ F_{max} & s < t < (m-1)s \\ \frac{F_{max}}{s}(9s - t) & (m-1)s < t < (m)s \end{cases} \quad (3)$$

Figure 3 shows an individual time-window for each cross-section along the ureter in order to be exposed to a piecewise linear force. Each time-window is dependent on the current time. Since each section is allocated to an individual time-window with a time span of 2-3 seconds, the force is applied to the cross-section when the current time reaches a particular time window.

| Section Number | Begin | End |
|---|---|---|
| n | (-m)s | 0 |
| n-1 | (-m+1)s | 1s |
| n-2 | (-m+2)s | 2s |
| n-m | 0 | ms |
| 1 | (-m+n-1)s | (n-1)s |

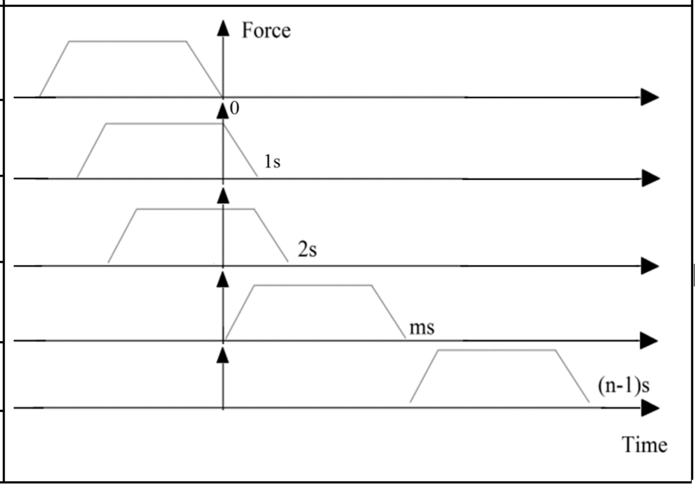


Figure 3: The piecewise linear function evaluated at *t* for different sections in the ureter.

## 2.6 Modelling of the Intra-Abdominal Pressure:

In order to prevent the ureter from excessive radial expansion, an Intra-Abdominal Pressure (IAP) model was introduced into the Y-code to model the IAP applied to the ureter in the native system. A detailed description of the algorithm is presented in Figure 4.

Max N is the maximum number of nodes in each cross-section of the structural mesh. To mimic IAP in the structural code, a force is applied to all nodes in the ureter's mesh at each time step. This method keeps the current coordinates of the centre of each cross-section the same as to the initial coordinates of the centre of each cross-section. The IAP is 4 $cmh_20$ in a healthy ureter. The magnitude offorce is obtained from the Eq (4) where *r* is the radius of the ureter, *L* is the length of the ureter and *N* is the number of surface nodes in the computational model.

$$\text{Force} = \text{IAP} \times \text{Area},\ \text{Area} = 2\pi rL/N,\ \text{Force} = 4000\ (\text{Braye}) \times 0.025\ (cm^2) = 100\ \text{Dynes} \quad (4)$$

Figure 5 (a-b) shows a comparison between the two computational models of the peristaltic movement in the presence and absence of the IAP. Figure 5(a) shows without the IAP, the ureter model is not constrained and starts moving in an eccentric direction. Figure 5(b) shows that with the presence of the IAP, the ureter model is fully constrained and the applied radial force leads to a centric contraction, similar to an actual human ureter.

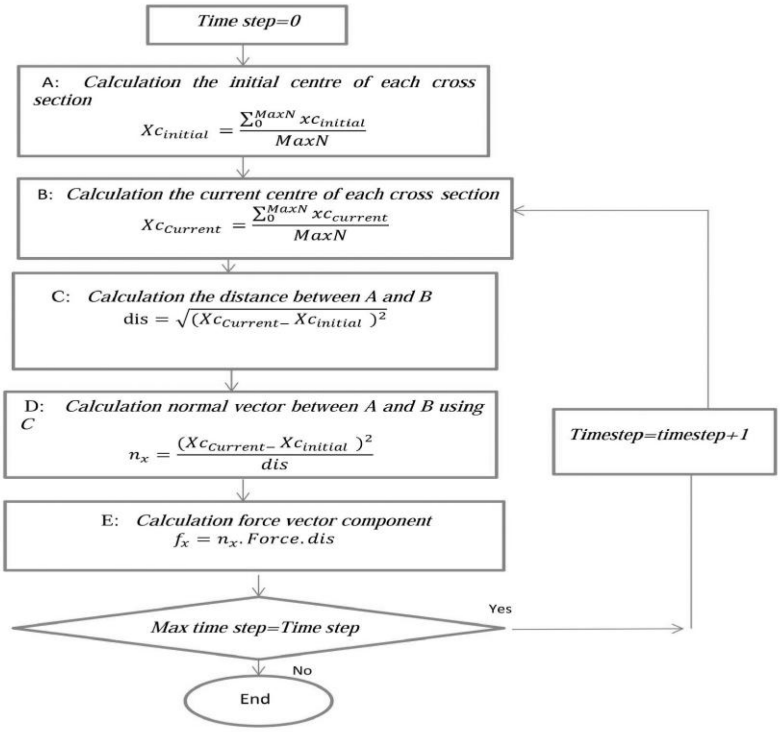


Figure 4: The IAP algorithm.

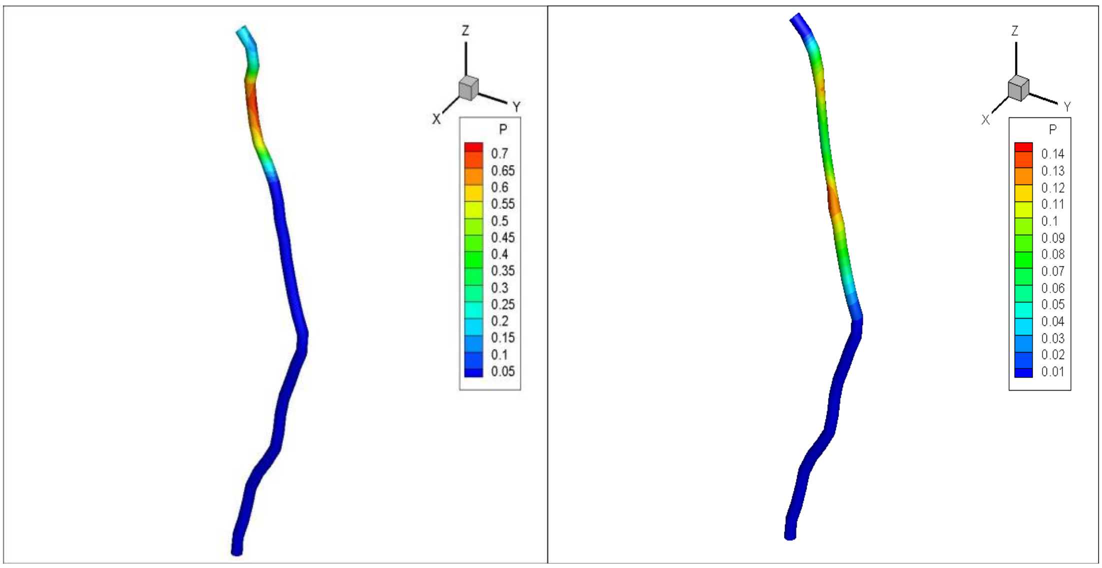


Figure 5: Comparison between the two simulations in the absence (a) and in the presence (b) of the IAP.

## 2.7 Boundary Conditions:

Urine is an incompressible Newtonian fluid with a dynamic viscosity coefficient of 0.01 Poise and a constant density of 1 g/cm$^3$. For this model, the initial velocity of urine in the ureter is taken as 0.01 cm/s. A no-slip boundary condition is applied between the urine and ureteral wall. Two different pressure differences are used between the inlet and outlet of the ureter to simulate a healthy ureteral contraction and depressed ureteral contraction under the effect of the relaxation drug. The aim of simulating a depressed ureteral contraction is to assess the possibility of reflux occurring during peristaltic movement in patients with an inadequate contraction force resulting from taking dilators. The pressure differences for the healthy and decreased ureteral contraction are extracted from a study by Shafik [10]. Table 1 shows the boundary conditions, contraction parameters and material properties of the simulations performed in this study.

Table 1: The boundary conditions, contraction parameters and material properties of the simulations performed in this work.

| Case studies | Conditions | Stress-strain relationship | Velocity of Contraction A and B (cm/s) | Pressure difference ($\nabla p$)/mmHg | Contraction Force (dyne) | IAP(dyne) |
|---|---|---|---|---|---|---|
| 1 | Healthy | Nonlinear | 3.5,1.75 | 0.5 | 1200 | 100 |
| 2 | Depressed ureteral contraction | Nonlinear | 3.5,3.5 | 0 | 450 | 100 |

In this study, a simulation of peristaltic movement was carried out by describing two pacemaker contractions, one in the proximal part of ureter (Contraction A) and one in the distal part of the ureter (Contraction B). The sections selected are shown in Figure 6. For the first case study, according to Kiil [20], the maximum pressure during the contraction is 25 mmHg. This is equivalent to force with the magnitude of 1200 dyne. The contractions move with a velocity between 1.5 to 3.5 cm/s [10, 20, 35]. The resting pressure difference between the inlet and the outlet is 0.5 mmHg [10]. For the second case study, a depressed ureteral contraction caused by taking dilators was simulated. As shown in previous clinical studies [36], the vasodilators drugs, used in promoting the passage of stones, lead to a highly depressed amplitude of the peristalsis. This results in a significant reduction in the ureteral contraction pressure between 20 to 65% [36]. For this study, to obtain a similar level of the depressed contraction pressure, a force of 450 is applied.

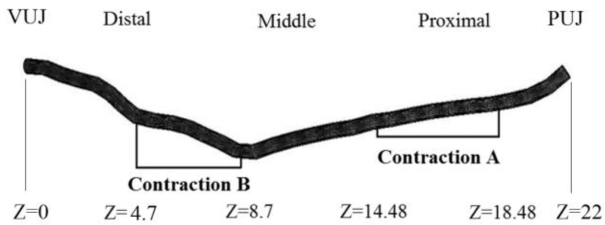


Figure 6: Contractions**A** and **B**which mimic pacemaker activities in the proximal and distal part of the ureter, Z is the distance along the ureter.

In figure 6 , Z is the distance along the ureter. The total length of the ureter is 22 cm. Z=22 is the Pelvis Ureteric Junction (PUJ) and Z=0 is the Vesico Ureteric Junction (VUJ). For the healthy condition, the contraction A starts from Z=18.8 cm and propagates towards Z=14.48 mm with a speed of 3.5 cm/s. Concurrently, Contraction B start at Z=8.7 mm and propagates towards Z= 4.7 mm with the same speed.

# 3 Results and Discussion

## 3.1 PLFM Results:

In order to verify the PLFM, a simulation of the contraction displacement in one ureteral cross–section was performed and the results were compared to the experimental data. Figure 7(a) shows the pressure using the PLFM in comparison with the experimental data extracted from the study by Kiil [20]. The resulting contact pressure from the area in which contraction force was applied, are digitally smoothed using a Savitzky–Golay filter. The maximum contact pressure is obtained by dividing the contact forces on each element by its area. Figure 7(a) shows that the PLFM produces a contact pressure with amplitude of 20 mmHg and a pulse duration of 2.3 seconds indicating a good agreement with the experimental ureteral pressure measurements [10, 20].

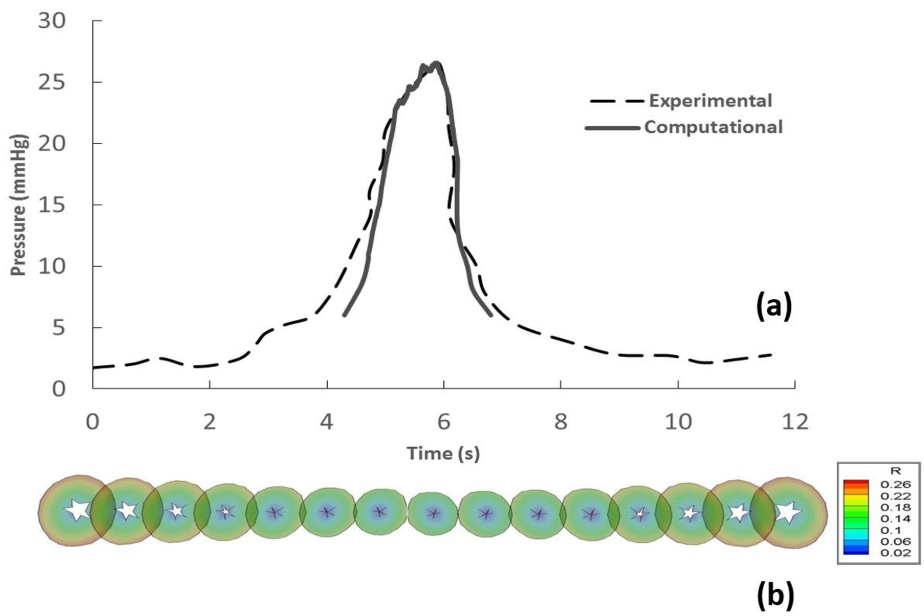


Figure 7: (a) The pressure time evolution using the PLFM in comparison with the experimental data extracted from the study by Kiil [20]. (b) The deformation of a cross-section over the same period of contraction time, where R is the radius displacement of the cross-section in cm.

Figure 7(b) shows the deformation of a cross-section over the same period of contraction time. R is defined as the radius displacement of the ureter in cm. This figure confirms the complete closure of the ureteral cross-section, where the maximum pulse pressure occurs. The pulse duration, shown in figure 7, is the time when the contact pressure increases to its maximum value and then gradually drops as the contraction travels away.The computational result from recording contact force is only compared with the part of the experimental result in which the ureteral wall are in contact. The advantage of using PLFM is to control the timing in contraction and relaxation of each cross-section

### 3.2 Simulation of a Healthy Ureteral Contraction:

A healthy ureter is simulated using the previously described boundary conditions. Figure 8 shows the wall shear stress at t=0.3, 0.6 and 1.0 s. The results show that, as expected, the shear stress is significantly higher around the contraction regions. It is clear that the highest shear stress occurs at the proximal part of the ureter, in the vicinity of the PUJ. The figure also shows that the maximum value of the shear stress decreases as the peristalsis propagates towards the VUJ.

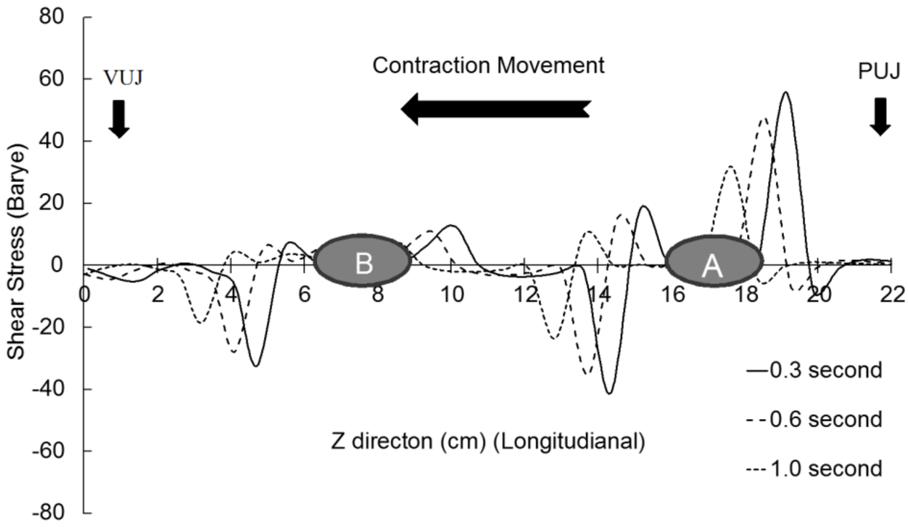


Figure 8: Longitudinal distribution (cm) of wall shear stress (Barye) that was computed with pressure difference of 0.6 $cmH_2o$ (healthy condition).

The results also show that the maximum shear stress on the wall depends on the velocity of the contraction in the ureter. The shear stress upstream of the Contraction B is 75% lower than that upstream of contraction A, because contraction B has a lower peristaltic velocity. These results show that the proximal part of ureter, in the vicinity of the PUJ, can be subject to a high shear stress and may result in a wall deformation. The occurrence of high shears stress at the proximal part of the ureter described by this study support the findings from other computational [23] and experimental studies [6]. This is indicative of large wall deformation and consequent proximal ureter rupture.

Figure 9 shows the average urine velocity at 0.5, 1.25, and 2.0 seconds for the healthy pressure difference condition. As the model steps from t = 0.5 to 2 seconds, the average reflux decreases by 85%. A similar drop in reflux as the contraction progresses has been reported in the study conducted byVahidi et al. [23]. The maximum speed of urine flow induced by the moving Contraction A varies between 3.3 to 3.5 cm/s and the maximum speed of urine flow induced by the moving Contraction B varies between 1.5 to 1.75 cm/s. So, it is concluded that when the complete closure of the cross-section occurs, the urine maximum velocity is very close to the contraction speed.

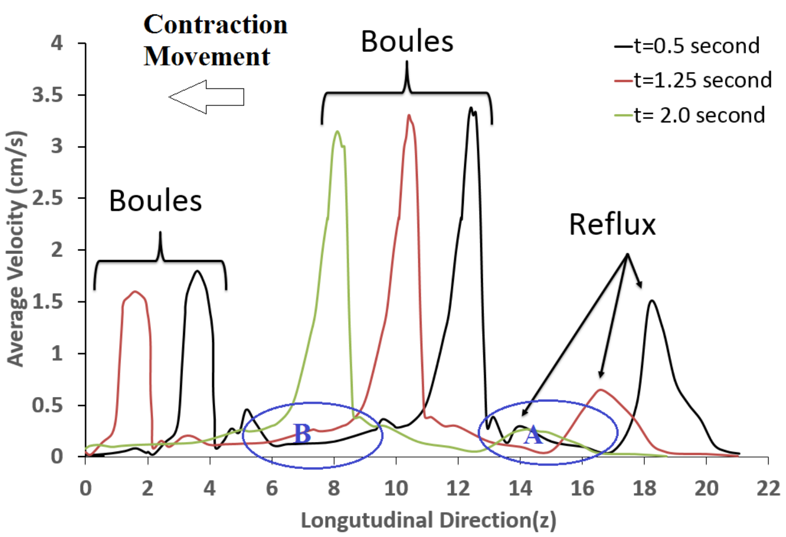


Figure 9: The average velocities of urine in the ureter using the model (t=0.5, 1.25, 2.0 seconds) in the healthy condition.

Figures 10 shows the urine velocity vectors behind the moving Contraction A at t = 0.5s. It is evident that there is a high, backward velocity, confirming the occurrence of a reflux upstream of the Contraction A.

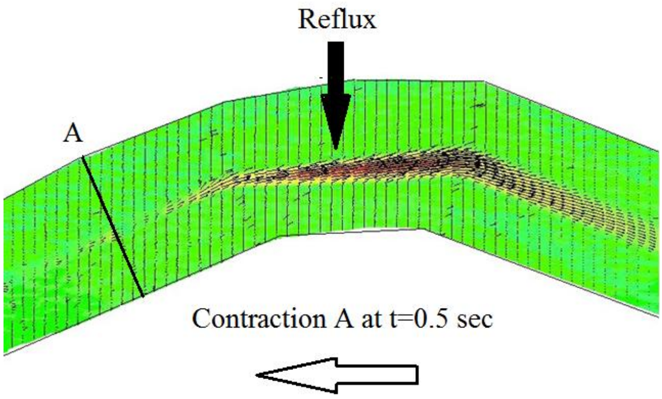


Figures 10: The urine velocity vectors behind the moving Contraction A at t= 0.5 second.

### 3.3 Simulation of a Depressed Ureteral Contraction:

Figure 11 shows the instantaneous velocity in the depressed ureteral contraction. The positive velocity represents the reflux and the negative velocity is the correct urine velocity in the direction of the contraction movement. The results indicate the presence of a continuous reflux upstream of the contraction during the peristaltic movement at t = 0.3, 1 and 2s. These results show that a patient taking dilators is more exposed to the risk of ureteric reflux. Although the urine velocity in this model is reduced by 75% compared to the healthy contraction, the reflux velocity almost remains unchanged. Since the average of ureteral diameter does not exceed than 0.5 cm, it can be concluded that the grade of the potential Vesicoureteric reflux (VUR) can be between grade 1 and 2. This means that the reflux can be limited to the ureter and up to the renal pelvis [37].

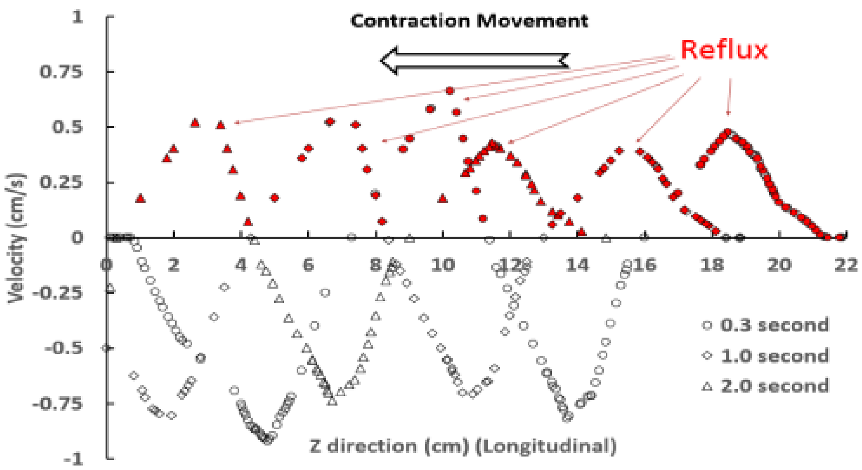


Figure 11: Instantaneous velocity profiles in Contractions A and B for the simulation of the unhealthy condition.

# 4 Conclusion

In this study, a novel peristalsis model is used to investigate the human ureter under two different conditions; a healthy contraction and a depressed ureteral contraction mimicking the effect of a relaxation drug. Realistic peristaltic motion of the ureter is modelled using a novel piecewise linear force function. It was shown that the piecewise linear force function produces a contact pressure in a good agreement with the experimental data. The results from the simulation of a depressed ureteral contraction show that the reflux occurring behind the contraction area remains unchanged as compared to the healthy condition. It was also found for both conditions that the high shear stress and reflux usually occur at the beginning of the lumen closure when the simulation starts. This gradually disappears due to the propagation of the peristalsis in which the lumen is completely closed by a contraction force. From this result it is indicated the initial location at which the pacemaker initiates the contraction, is crucial. Since the pacemakers are located at multiple sites in the upper urinary tract, it can be concluded that not all peristalsis movements cause high reflux or high shear stresses in the proximal part of the ureter. This still leaves many questions unresolved. For instance, the nature of the reflux, which is one of the biggest challenges in urodynamic research, is not still clear enough to be simulated. The interaction between the kidney and bladder pressure has hardly received any theoretical or numerical simulations and deserves further invetigation.

# 5 Conflict of Interest and Human Subjects

None.

# 6 Acknowledgement:

National computing time was provided by **UK Turbulence Consortium** under EP SRC grant EP/L000261,
Clinical data was provided by urology research innovation at Whipps cross Hospital

# 7 References:

[1] A.J. Wein, L. Kavoussi, W. Partin, and C.A. Peters. Urology, Campbell-Walsh. "vol. 2 of." *Section XIV*(2012).

[2 ]Weiss, R. M., M. L. Wagner, and B. F. Hoffman. "Localization of the pacemaker for peristalsis in the intact canine ureter." *Invest Urol* 5.42 (1967): 1.

[3] Osman, Fares, et al. "A novel videomicroscopic technique for studying rat ureteral peristalsis in vivo." *World journal of urology* 27.2 (2009): 265-270.

[4] Yin, F. C., and Y. C. Fung. "Mechanical properties of isolated mammalian ureteral segments." *American Journal of Physiology--Legacy Content* 221.5 (1971): 1484-1493.

[5] Watanabe, Hiroki, Yuji Nakagawa, and Mutsumi Uchida. "Tests to evaluate the mechanical properties of the ureter." *Biomaterials' Mechanical Properties*. ASTM International, 1994.

[6] Sokolis, Dimitrios P., et al. "Age-and region-related changes in the biomechanical properties and composition of the human ureter." *Journal of biomechanics* 51 (2017): 57-64.

[7 ] Eken, Alper, Tugana Akbas, and Taner Arpaci. "Spontaneous rupture of the ureter." *Singapore medical journal* 56.2 (2015): e29.

[8] Choi, Seung-Kwon, et al. "A rare case of upper ureter rupture: ureteral perforation caused by urinary retention." *Korean journal of urology* 53.2 (2012): 131-133.

[9] Woodside, J. R., and T. A. Borden. "The pressure-flow relationship of the normal ureter." *Investigative urology* 18.1 (1980): 82-83.

[10] Shafik, Ahmed. "Ureteric profilometry: a study of the ureteric pressure profile in the normal and pathologic ureter." *Scandinavian journal of urology and nephrology* 32.1 (1998): 14-19.

[11] Irina, Mudraya, and Khodyreva Lubov. "Ureteric function and upper urinary tract urodynamics in patients with stones in kidney and ureter." *Evolving Trends in Urology*. InTech, 2012.

[12] Tillig, Bernd, and Christos E. Constantinou. "Videomicroscopic imaging of ureteral peristaltic function in rats during cystometry." *Journal of pharmacological and toxicological methods* 35.4 (1996): 191-202.

[13] Lewis, C. A., et al. "Radionuclide imaging of ureteric peristalsis." *BJU International* 63.2 (1989): 144-148.

[14] Patel, U., and M. J. Kellett. "Ureteric drainage and peristalsis after stenting studied using colour Doppler ultrasound." *BJU International* 77.4 (1996): 530-535.

[15] Roshani, H., et al. "An in vivo endoluminal ultrasonographic study of peristaltic activity in the distal porcine ureter." *The Journal of urology* 163.2 (2000): 602-606.

[16] Venkatesh, Ramakrishna, et al. "Impact of a double-pigtail stent on ureteral peristalsis in the porcine model: initial studies using a novel implantable magnetic sensor." *Journal of endourology* 19.2 (2005): 170-176.

[17] Roshani, H., et al. "A study of ureteric peristalsis using a single catheter to record EMG, impedance, and pressure changes." *Techniques in urology* 5.1 (1999): 61-66.

[18] Ulmsten, Ulf, and Jan Diehl. "Investigation of ureteric function with simultaneous intraureteric pressure recordings and ureteropyelography." *Radiology* 117.2 (1975): 283-289..

[19] Young, Anthony J., et al. "Evaluation of novel technique for studying ureteral function in vivo." *Journal of endourology* 21.1 (2007): 94-99

[20] Kiil, Fredrik. "FUNCTION OF THE URETER AND RENAL PELVIS." *Annals of Surgery* 148.2 (1958): 280-291.

[21] Manton, M. J. "Long-wavelength peristaltic pumping at low Reynolds number." *Journal of Fluid Mechanics* 68.3 (1975): 467-476.

[22] Zien, T-F., and S. Ostrach. "A long wave approximation to peristaltic motion." *Journal of Biomechanics* 3.1 (1970): 63-75.

[23] Vahidi, Bahman, and Nasser Fatouraee. "A numerical simulation of peristaltic motion in the ureter using fluid structure interactions." *Engineering in Medicine and Biology Society, 2007. EMBS 2007. 29th Annual International Conference of the IEEE*. IEEE, 2007.

[24] Xiao, Q., and M. Damodaran. "A numerical investigation of peristaltic waves in circular tubes." *International Journal of Computational Fluid Dynamics* 16.3 (2002): 201-216.

[25] Kumar, BV Rathish, and K. B. Naidu. "A numerical study of peristaltic flows." *Computers & fluids* 24.2 (1995): 161-176.

[26] Vahidi, Bahman, et al. "A mathematical simulation of the ureter: effects of the model parameters on ureteral pressure/flow relations." *Journal of biomechanical engineering* 133.3 (2011): 031004.

[27] Vahidi, Bahman, et al. "A mathematical simulation of the ureter: effects of the model parameters on ureteral pressure/flow relations." *Journal of biomechanical engineering* 133.3 (2011): 031004.

[28] Woodburne, Russell T., and Jack Lapides. "The ureteral lumen during peristalsis." *Developmental Dynamics* 133.3 (1972): 255-258.

[29] G. Hosseini, Ghazaleh, et al. Computational simulation of the urinary system. Proceedings of the world congress on Engineering and Computer Science Vol II, (2012) ISBN: 978-988-19252-4-4

[30]. Hosseini, Ghazaleh, et al. "Simulation of the upper urinary system." *Critical Reviews™ in Biomedical Engineering* 41.3 (2013).

[31] Thomas, T. G., and J. J. R. Williams. "Development of a parallel code to simulate skewed flow over a bluff body." *Journal of wind engineering and industrial aerodynamics* 67 (1997): 155-167.

[32] Ji, C., A. Munjiza, and J. J. R. Williams. "A novel iterative direct-forcing immersed boundary method and its finite volume applications." *Journal of Computational Physics* 231.4 (2012): 1797-1821.

[33] Munjiza, Antonio A. *The combined finite-discrete element method*. John Wiley & Sons, 2004..

[34] Singh, K. M., et al. "On parallel pre-conditioners for pressure Poisson equation in LES of complex geometry flows." *International Journal for Numerical Methods in Fluids* 83.5 (2017): 446-464.

[35]. Boyarsky, Saul, Carl W. Gottschalk, and Emil A. Tanagho. *Urodynamics: hydrodynamics of the ureter and renal pelvis*. Academic Press, 2014.

[36] Davenport, Kim, Anthony G. Timoney, and Francis X. Keeley Jr. "The role of ureteral relaxation in the promotion of stone passage." *AIP Conference Proceedings*. Vol. 900. No. 1. AIP, 2007.

[37] Arlen, Angela M., et al. "Validation of the ureteral diameter ratio for predicting early spontaneous resolution of primary vesicoureteral reflux." *Journal of Pediatric Urology* (2017).